

Voice Coil Impedance as a Function of Frequency and Displacement

Mark Dodd¹, Wolfgang Klippel², and Jack Oclee-Brown.³

¹ KEF Audio UK (Ltd), Maidstone, Kent, ME15 6QP United Kingdom.
Mark.dodd@KEF.com

² Klippel GmbH, Dresden, 02177, Germany.
wklippel@klippel.de

³ KEF Audio UK (Ltd), Maidstone, Kent, ME15 6QP United Kingdom.
Jack.oclee-brown@KEF.com

ABSTRACT

Recent work by Klippel [1] and Voishvillo [2] has shown the significance of voice coil inductance in respect to the non-linear behaviour of loudspeakers. In such work the methods used to derive distortion require the inductance to be represented by an equivalent circuit rather than the frequency domain models of Wright and Leach. A new technique for measurement of displacement and frequency dependant impedance has been introduced. The complex relationship between coil impedance, frequency and displacement has been both measured and modelled, using FE, with exceptional agreement. Results show that the impedance model requires that its parameters vary independently with x to satisfactorily describe all cases. Distortion induced by the variation of impedance with coil displacement is predicted using both parameterised and FE methods, these predictions are compared to measurements of the actual distortion. The nature of this distortion is discussed.

1. INTRODUCTION

In order to describe the performance of a loudspeaker precisely, one must consider the electrical input impedance at higher frequencies. The voice coil does not operate in free air but close to conducting and magnetically permeable structures: the pole tips, the magnet, the voice coil former, copper rings etc. The impedance can be only roughly modelled as a resistor R_e and an ideal inductance L_e , the occurrence of eddy currents in these structures usually decreases the inductance of the coil and increases losses at higher frequencies [3].

The nature of the voice coil impedance is dependent upon the geometry and physical properties of the magnet and surrounding assemblies. There are three prominent methods of deducing the coil (blocked) impedance for a particular loudspeaker.

- The blocked impedance may be measured by clamping the voice coil stationary within the magnet assembly to remove the motional part of the impedance. Blocked impedance may then be measured as with conventional impedance measurements.
- Various impedance models have been developed in order to describe the electrical behaviour of the coil, these models may be fitted to conventional unblocked impedance measurements.
- Recently magnetic transient FEM has been successfully applied to deduce the blocked impedance [4].

At large amplitudes the impedance also varies significantly with voice coil displacement. Whereas the frequency dependence of the impedance is a linear phenomenon effecting the amplitude response, but not generating distortion, variation of impedance with displacement generates significant harmonic and inter-modulation distortion.

The nature of the impedance generated distortion is a dependent upon the coil impedance, or more precisely how the coil impedance varies with frequency & displacement of the coil.

This paper investigates the voice coil impedance as a function of frequency and of displacement. Measurements of frequency & displacement dependent impedance have been made using a quasi-static method using the LPM module of the Klippel analyser [5]. Frequency & displacement dependent impedance has

also been predicted using FEM analysis. A new impedance model with displacement varying parameters is discussed and fitted to the measured data. Finally, distortion induced by the variation of impedance with coil displacement is predicted using both parameterised and FE methods, these predictions are compared to measurements of the actual distortion. The nature of this distortion is discussed.

1.1. Glossary

| | |
|-----------------------------|--|
| $Bl(x)$ | force factor (Bl product) |
| $C_{ms}(x) = 1 / K_{ms}(x)$ | mechanical compliance of loudspeaker suspension |
| Exm | exponent of imaginary part in WRIGHT model |
| Erm | exponent of real part in WRIGHT model |
| $F_m(x,i)$ | reluctance force |
| Krm | factor of real part in WRIGHT model |
| Kxm | factor of imaginary part in WRIGHT model |
| K | factor in LEACH model |
| $K_{ms}(x)$ | mechanical stiffness of loudspeaker suspension |
| $L_e(x)$ | inductance used (cascaded model) |
| $L_2(x)$ | inductance (cascaded model) |
| $L_{eff}(f,x)$ | effective inductance depending on |
| M_{ms} | mechanical mass of loudspeaker diaphragm assembly including air load and voice coil |
| n | exponent in LEACH model |
| R_{ms} | mechanical resistance of total-loudspeaker |
| R_e | electrical voice coil DC-resistance |
| $R_2(x)$ | resistance (cascaded model) |
| $R_{eff}(f,x)$ | effective losses due to eddy currents depending on frequency and displacement |
| $Z_L(j\omega,x)$ | complex excess impedance representing the effect of the lossy inductance (motional impedance and R_e is removed) |
| ω | angular frequency $\omega = 2\pi f$ |

2. MODELLING

2.1. Lumped Parameter Model

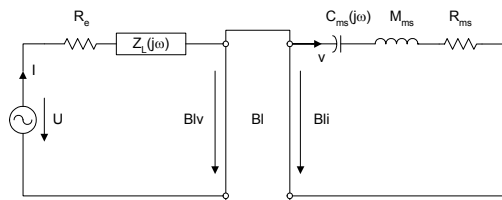


Figure 1 Electro-mechanical equivalent circuit of the loudspeaker

Figure 1 shows a simple equivalent circuit of a loudspeaker system. The dominant nonlinearities are the variation of the force factor $Bl(x)$, the mechanical compliance $C_{ms}(x)$ and the electrical impedance $Z_L(j\omega, x)$ with voice coil displacement x . The DC resistance R_e and the motional impedance are not considered in the electrical impedance $Z_L(j\omega, x)$. Thus the impedance $Z_L(j\omega, x)$ may be measured at the electrical terminals by blocking the movement of the coil and subtracting the resistance measured at a very low frequency.

Different linear models have been developed to describe the frequency dependency of $Z_L(j\omega, x)$ with a minimal number of free parameters:

2.1.1. LEACH model

M. Leach [6] proposed a weighted power function of the complex frequency as an approximation for Z_L

$$Z_L(j\omega) = K \cdot (j\omega)^n; \quad \omega = 2\pi f \quad (1)$$

Although using only two free parameters this function can sometimes give a very good fit over a wide frequency range. Unfortunately, this function can not be represented by an electrical equivalent circuit nor a simple digital system.

2.1.2. LR-2 Model

This model uses a series inductance L_e connected to a second inductance L_2 shunted by resistance R_2 .

$$Z_L(j\omega) = L_e j\omega + (R_2 L_2 j\omega) / (R_2 + L_2 j\omega) \quad (2)$$

Although this model uses three free parameters it often provides a worse fit to measured Z_L than the LEACH model. However, this model may be realised as an

electrical equivalent circuit (as shown in Figure 2 b) or as a digital IIR filter.

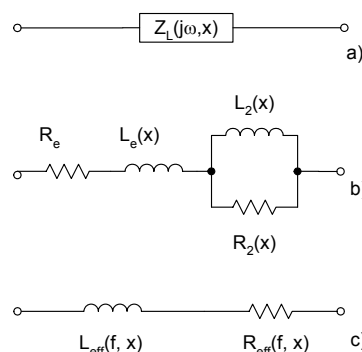


Figure 2 Representation of the electrical impedance

2.1.3. WRIGHT model

Wright [7] proposed a model using separate weighted power functions in ω for both the real and imaginary part of impedance.

$$Z_L(j\omega) = K_{rm} \cdot \omega^{Erm} + j \cdot (K_{xm} \cdot \omega^{Exm}) \quad (3)$$

This model uses four free parameters and normally gives a better fit than the other models with less parameters. Unfortunately, this function can not be directly realised as an analogue or digital system.

2.1.4. Effective inductance

$$Z_L(j\omega) = L_{eff}(f)j\omega + R_{eff}(f) \quad (4)$$

M. Leach also proposed normalising the imaginary part of the electrical impedance $Z_L(j\omega)$ to the frequency $j\omega$ and introducing an effective inductance $L_{eff}(f)$ which varies with frequency. The real part of $Z_L(j\omega)$ may be considered as a frequency depending resistance $R_{eff}(f)$ describing the losses due to eddy currents as shown in Figure 2c. Though the number of parameters is very high, two parameters for each frequency point, both parameters are easy to interpret and convenient for graphical representation.

2.1.5. Large signal modelling

The linear models may be easily expanded to higher amplitudes by allowing each parameter to be dependent upon the displacement x .

For example considering the LR-2 model, the three parameters $L_e(x)$, $R_2(x)$ and $L_2(x)$ are functions of the

displacement x and may be approximated by a truncated power series expansion such as

$$L_e(x) = \sum_{i=0}^N l_i x^i \quad (5)$$

$$R_2(x) = \sum_{i=0}^N r_i x^i \quad (6)$$

$$L_2(x) = \sum_{i=0}^N \lambda_i x^i \quad (7)$$

where the coefficients l_i , r_i and λ_i are the free parameters of the model.

3. MEASUREMENT

The application of a model to a particular real object usually requires an estimation of the free model parameters in such a way that the model describes the real object with maximal accuracy.

With the linear models straightforward techniques are available which may be applied for loudspeakers at small amplitudes.

Non-linear models require special techniques for the parameter identification. Static, quasi-static and full dynamic techniques have been developed to measure the force factor $Bl(x)$, compliance $C_{ms}(x)$ and inductance parameter $L_e(x)$. The dynamic techniques have the advantage that an audio-like ac signal is used for excitation and the loudspeaker is operated under working conditions.

The current version of the LSI module in the Klippel analyser performs a dynamic measurement using a noise stimulus [8]. The free model parameters are optimised to give the best fit between measured and modelled current and displacement. The LR-2 model is currently constrained so that the three lumped parameters vary with the same shape in x .

$$\frac{L_e(x)}{L_e(0)} \approx \frac{R_2(x)}{R_2(0)} \approx \frac{L_2(x)}{L_2(0)} \quad (8)$$

Although this assumption is a good approximation for most loudspeakers without shorting rings it is a purpose of the paper to investigate the validity of this approximation for more elaborate loudspeakers using copper cups and aluminium rings for reducing the inductance nonlinearity.

Clearly the measurement of suspension stiffness using a dc offset gives significantly different results from a dynamic measurement due to creep, relaxation and other time dependent properties. Additionally, due to flux modulation, the force factor $Bl(x)$ and the inductance $L_e(x)$ are dependent on the current i . Thus using an audio-like signal will produce far more meaningful data than measurement with extremely small input current (coil offset generated by external force or pressure) or extremely large currents (coil offset generated by a dc current).

Despite these limitations a quasi-static technique is a useful method for investigating the variation of the impedance with both frequency and displacement.

Measurements have been performed on two test loudspeakers. Both loudspeakers share the following specifications:

Voice coil diameter: 2" nominal (51.30mm ID)
 Voice coil DCR: 6.72 Ohms
 Turns in Voice coil: 126 Turns
 Ferrite ring magnet
 Annular low carbon steel top-plate
 Pole/plate assembly type yoke.

The magnet assembly of loudspeaker 1 has an aluminium shorting ring placed above the magnetic gap. The magnetic assembly of loudspeaker 2 has an aluminium shorting ring placed below the magnetic gap. The geometry of the two loudspeakers is shown in Figure 26 & Figure 27. The pair serve to illustrate the influence of the effect of aluminium rings on the variation of the voice coil inductance with displacement.

3.1. Mechanical Setup

A method for measurement of the displacement dependent impedance was developed at GP Acoustics (UK). The method is a simple modification to the standard Linear Parameter Measurement (LPM) of the KLIPPEL Analyser system. The measurements presented in this paper were performed by Klippel GmbH.

The loudspeaker is clamped in vertical position in the professional loudspeaker stand as shown in Figure 3.

An additional spider is attached to the diaphragm.

The spider holds an inner clamping part made of aluminium which is secured to the lower rod (usually used for holding the microphone).

By shifting the lower rod a displacement may be imposed to the coil position. Clearly displacing the coil

will also change the other parameters such as $Bl(x)$, $C_{ms}(x)$ and also loss factors.

The Distortion Analyser also provides a Displacement Meter ([5] Hardware) this is used for measuring the original rest position of the cone and to measure the imposed static displacement. Throughout this paper the convention is that a positive displacement of the coil refers to movement out of the magnet assembly.

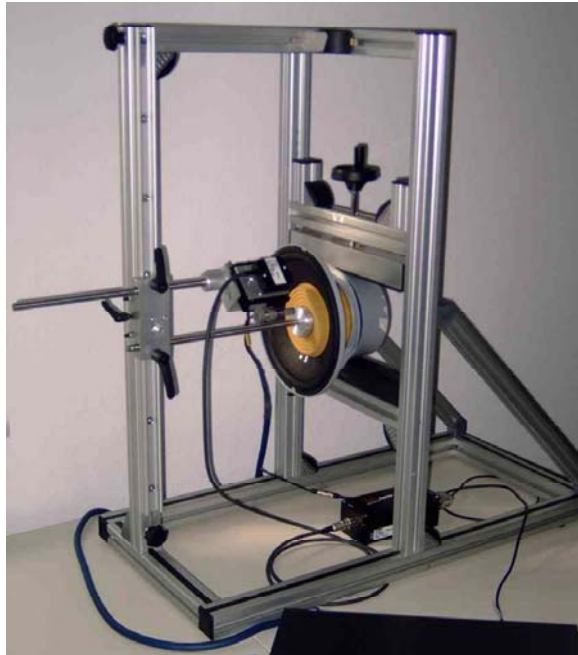


Figure 3 Measurement Setup.

The loudspeaker under test is connected to Distortion Analyser 2 allowing a simultaneous measurement of voltage, current and displacement signal.



Figure 4 Generating an additional DC offset by the lower rod connected by an addition spider to the diaphragm.

3.2. Small signal measurements

The additional spider increases the stiffness of the total suspension and the resonance frequency. However, the modified loudspeaker is still a second-order system and can be represented by the equivalent circuit in

Figure 1.

The module Linear Parameter Measurement (LPM) of the KLIPPEL Analyser system is used to measure the linear parameter at each prescribed displacement.

The loudspeaker is excited by a multitone signal of 0.5 V rms at the terminals. Since the voltage, current and displacement are measured simultaneously all of the linear parameters can be identified instantaneously. An additional measurement with a mechanical perturbation (additional mass or measurement in a test enclosure) is not required.

A sparse multitone signal used as excitation signal allows assessment of the distortion generated by the loudspeaker. During the small signal measurements the maximum distortion occurred 20 dB below the fundamental lines in the current spectrum. This shows sufficiently linear operation of the loudspeaker [9].

3.3. Fitting of the inductance model

At first the linear parameters are measured at the rest position ($x=0$) and the different inductance models (LR-2, WRIGHT, LEACH) are used to describe the impedance response, measured up to 18 kHz.

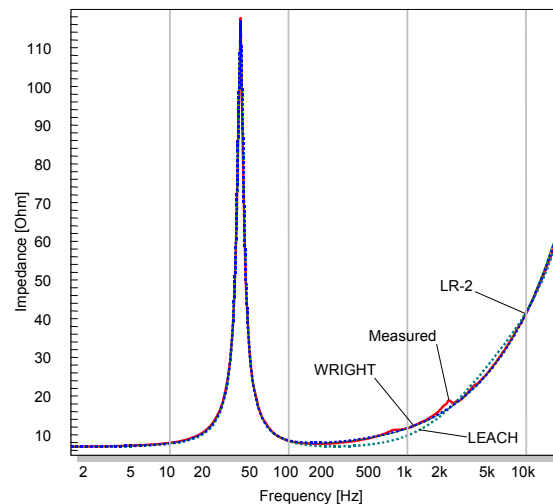


Figure 5 Magnitude of electrical impedance of loudspeaker 1 measured and fitted by LR-2, Wright and LEACH model up to 18 kHz.

Figure 5 shows a measured curve and the fitted curves using the three models. The LEACH and WRIGHT are able to describe this particular impedance curve very well. The LR-2 causes minor deviations about 500 Hz and 5 kHz. Although the WRIGHT usually gives the best fit there are cases where the other models have provided a superior fit.

Since the test loudspeaker is based on a woofer intended for frequencies below 200 Hz the models are have also been fitted using data only up to 2 kHz, Figure 6. In this instance all models are able to give a good fit to the measured curve.

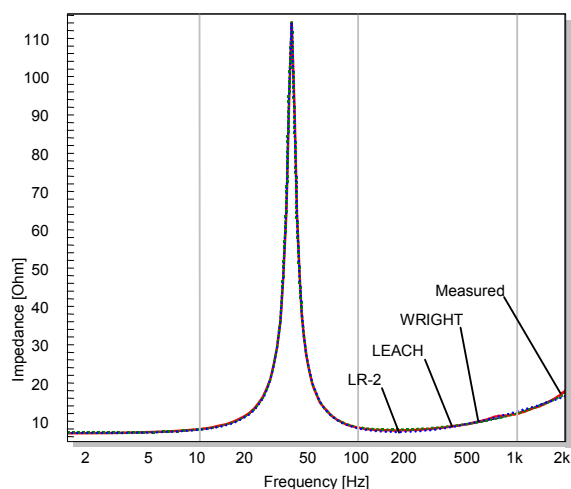


Figure 6 Magnitude of electrical impedance of loudspeaker 1 measured and fitted by LR-2, WRIGHT and LEACH model up to 2 kHz.

3.4. Excess impedance Z_L

The LPM module also calculates the amplitude and phase response of the excess impedance $Z_L(j\omega)$. The measured and the fitted curves are shown in Figure 7 using the LEACH model. The measured curves are calculated by subtracting the estimated dc resistance R_e and the motional impedance (calculated from the estimated parameters Bl , M_{MS} , R_{MS} , and C_{MS}) from the total electrical input impedance. The magnitude increases with frequency, normally with a slope usually less than 6 dB per octave. The LEACH model uses a constant slope corresponding with the exponent n in Equation (1). Close to loudspeaker resonance the magnitude of the calculated excess impedance varies significantly. In this region the motional impedance is very high (~100 Ohm), measurement and modelling error (in the order of 1 %) will be assigned to the excess impedance and makes accurate estimation of the excess

impedance below 100 Hz impossible. The calculated phase of the excess impedance is about 68 degrees with a small decay to higher frequencies. The LEACH model assumes a constant phase, which proves to be a good approximation for this particular loudspeaker.

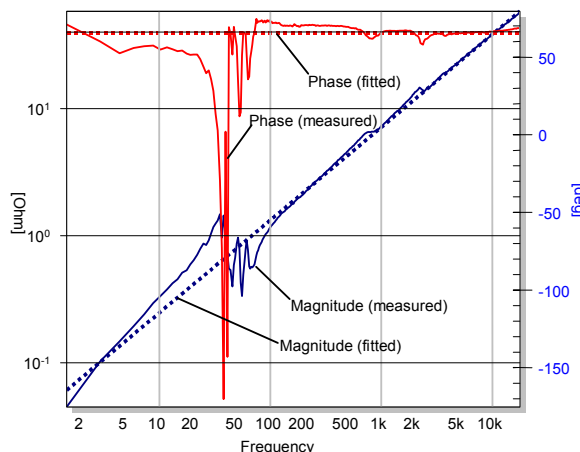


Figure 7 Magnitude and phase of the electrical impedance of loudspeaker 1 $Z_L(j\omega)$ measured (solid lines) and fitted by using the LEACH model (dotted lines).

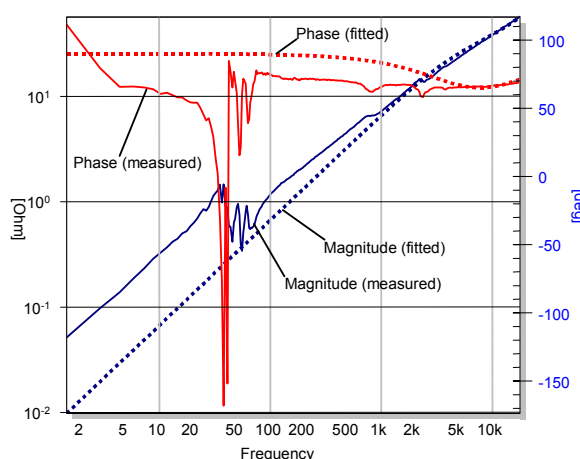


Figure 8 Magnitude and phase of the electrical impedance $Z_L(j\omega)$ of loudspeaker 1 measured (solid lines) and fitted by using the LR-2 model (dotted lines).

Figure 8 shows the excess impedance match using the LR-2 model. While the fitting above 1 kHz is good, at lower frequencies there are significant differences in both phase and amplitude. The LR-2 model, and also other shunted models using more L_i and R_i elements ($i > 2$), behaves as an ideal inductance at very low frequencies giving a 6dB per octave slope and a phase shift of 90 degrees. This property corresponds with the observation that the eddy currents are frequency

dependent and will vanish at very low frequencies. Though a small increase in the measured phase at low frequencies supports this observation, the phase shift of the LR-2 model begins at a higher frequency than the measured shift. Thus the LR-2 is usually limited to use over a frequency band of two decades. Using an additional shunted section (R_3 and L_3) improves the fit significantly and results in a good description over the whole audio band (three decades). The cascade of shunted inductances is a minimum-phase system and can be realised in the analogue or digital domain.

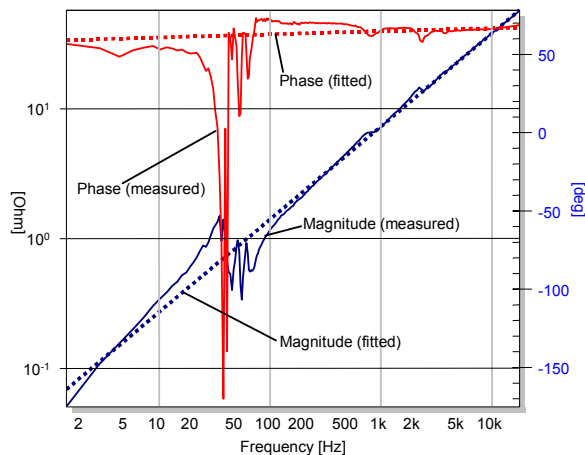


Figure 9 Magnitude and phase of the electrical impedance $Z_L(j\omega)$ of loudspeaker 1 measured (solid lines) and fitted by using the WRIGHT model (dotted lines).

The excess impedance fitted by the WRIGHT model is shown in Figure 9. The magnitude response can be approximated by smooth line having a different slope at low and high frequencies (corresponding with exponents E_{rm} and E_{xm}). Contrary to the LEACH model the phase is not constant but depends on all four parameters. The WRIGHT model also considers the response below 100 Hz, where measurement errors and noise have corrupted the measurement, and generates a decrease of phase shift at very low frequencies. Since the WRIGHT model is not bounded to be minimum phase and not composed from a system lumped electrical elements it may be deceived by measurement artefacts when used to represent a measured curve. Thus a good match with the measured impedance curve does not guarantee that the parameters are meaningful.

3.5. Impedance versus displacement

Once measurements had been performed at rest position ($x=0$) a dc offset was imposed upon the coil using the lower rod in Figure 4. The Displacement Meter at the

hardware unit, Distortion Analyser 2, was used to measure the offset. The LPM module was then again used to measure the linear parameters. The excess impedance Z_L is displayed for loudspeaker 1 in Figure 10 for a negative offset of -8mm (coil in) and a positive offset of 7.5mm (coil out), the impedance at the rest position is also shown. The variation of the impedance with displacement may be clearly seen. It may be observed that the inductance of the coil is effectively reduced in the region near to the aluminium shorting rings, above the gap in this case. Conversely as the coil moved into the magnetic assembly, the effective inductance is increased as the coil moves away from the pole piece and top plate.

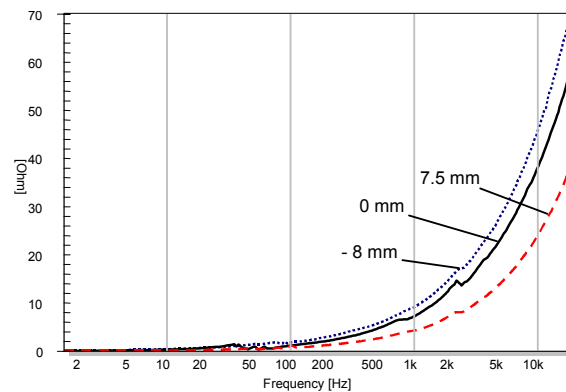


Figure 10 Magnitude of electrical impedance $Z_L(j\omega)$ of Loudspeaker 1 measured at rest position (solid line), at -8 mm (dotted line) and 7.5 mm (dashed line)

The phase of the excess impedance Z_L was also calculated and is shown in Figure 11 at the same coil positions. Whereas the impedance magnitude varies by up to 40 % at higher frequencies the phase stays almost constant at 70 degrees.

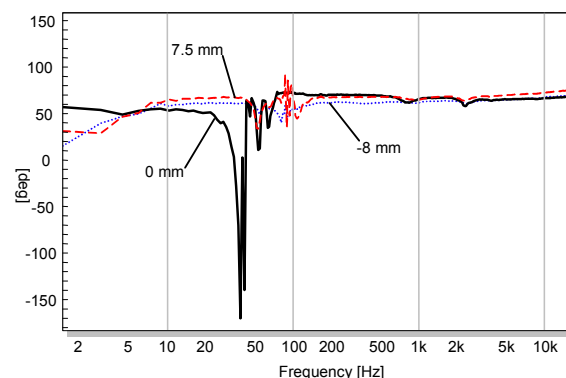


Figure 11 Phase of electrical impedance $Z_L(j\omega)$ of Loudspeaker 1 measured at rest position (solid line), at -8 mm (dotted line) and 7.5 mm (dashed line)

3.6. Non-linear Parameters

Having identified the linear parameters for different values of coil offset, the displacement dependency of the parameters were be calculated using the Math Processing Software (MAT), a free programmable (SCILAB or MATLAB) module [10] for the KLIPPEL Analyser. This module imports all of the results measured by the LPM for all measured voice coil offsets and calculates the coefficients l_i , r_i and λ_i in equations (5) - (7).

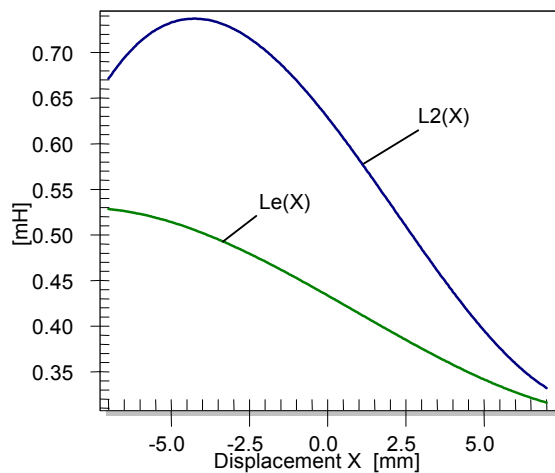


Figure 12 Inductance $L_e(x)$ and $L_2(x)$ of loudspeaker 1 versus displacement x .

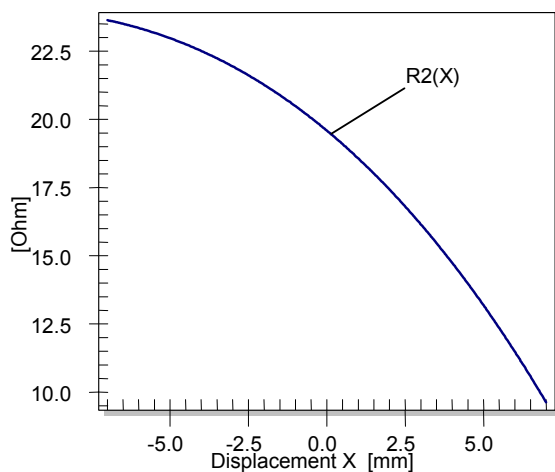


Figure 13 Resistance $R_2(x)$ of loudspeaker 1 versus displacement x .

Figure 12 and Figure 13 show the parameters $L_e(x)$, $L_2(x)$ and $R_2(x)$ of the LR-2 model versus displacement x for loudspeaker 1 (ring above the gap). The LR-2 model is used as the parameters have an analogue

representation and are easy to interpret. Corresponding to our observations regarding the measured excess impedance, it can be seen that the fitted model also identifies the effective inductance as reducing when the coil is close the aluminium shorting ring above the magnetic gap. It is interesting to observe that the shape of the parameter functions; $L_e(x)$, $R_2(x)$ and $L_2(x)$; is very similar in this instance. In this case the assumption of (8) appears to be valid.

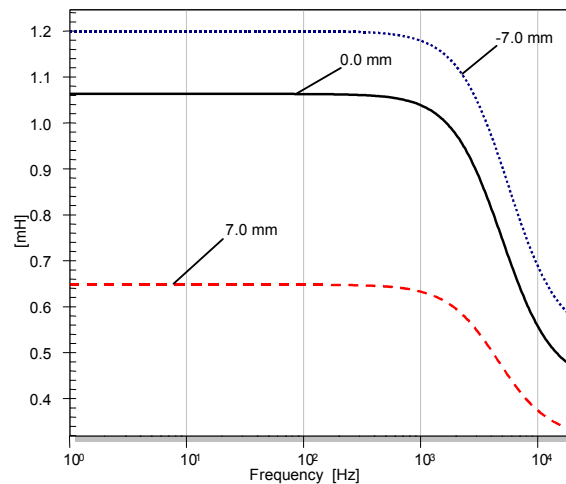


Figure 14 Effective inductance $L_{eff}(f,x)$ versus frequency f of loudspeaker 1 plotted for the rest position (solid line) and -7 and $+7$ mm displacement (dotted and dashed line, respectively).

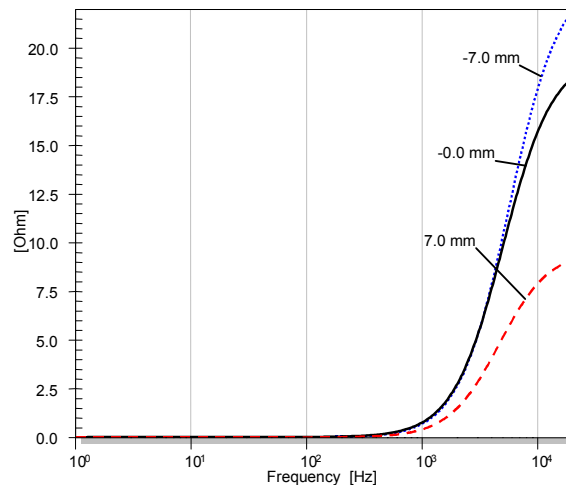


Figure 15 Effective resistance $R_{eff}(f,x)$ versus frequency f of loudspeaker 1 plotted for the rest position (solid line) and -7 and $+7$ mm displacement (dotted and dashed line, respectively).

Use of the effective resistance $R_{eff}(f,x)$ and the effective inductance $L_{eff}(f,x)$, as defined in equation (4) and illustrated in Figure 2 c, simplifies interpretation of the

excess impedance. Figure 14 shows the effective inductance $L_{eff}(f,x)$ for three different voice coil displacements based on the LR-2 model. It is clearly shown that the voice coil inductance decreases if the coil moves outwards and increases as the coil moves in.

At low frequencies the effective inductance $L_{eff}(f,x)$ is equal to the sum of $L_e(x)$ and $L_2(x)$ and the effective resistance $R_{eff}(f,x)$, Figure 15, is close to zero. At high frequencies the $L_{eff}(f,x)$ is equal to $L_e(x)$ only and the effective resistance $R_{eff}(f,x)$ becomes equal to $R_2(x)$.

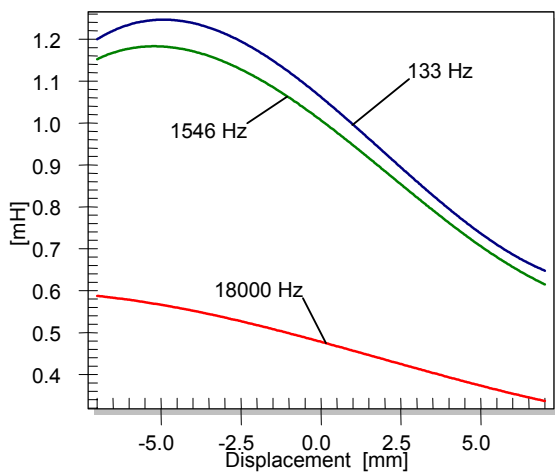


Figure 16 Effective inductance $L_{eff}(f,x)$ versus displacement x of loudspeaker 1 plotted for frequencies 133 Hz, 1545 Hz and 18 kHz.

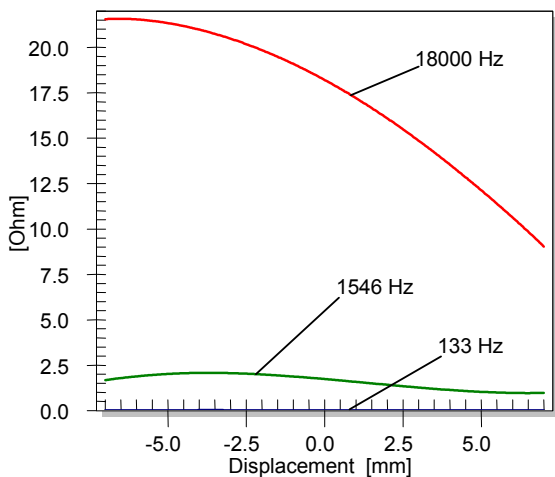


Figure 17 Effective resistance $R_{eff}(f,x)$ versus displacement x of loudspeaker 1 plotted for frequencies 133 Hz, 1545 Hz and 18 kHz.

Figure 16 and Figure 17 shows the variation of effective inductance and resistance versus displacement x for selected frequencies 133Hz, 1545Hz and 18kHz. Clearly all the curves have a distinct asymmetry and decrease with positive displacement.

A second loudspeaker has been made using the same suspension and motor structure but with the aluminium ring located below the magnetic gap.

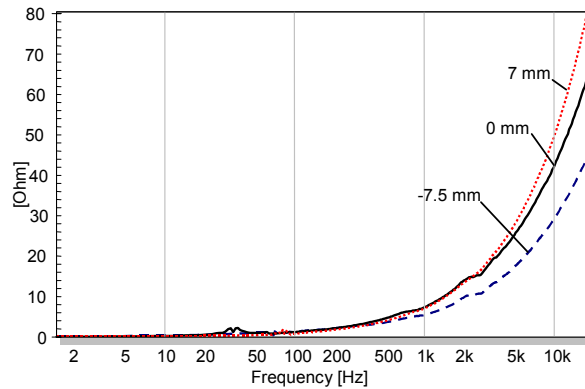


Figure 18 Magnitude of electrical impedance $Z_L(jw)$ of loudspeaker 2 (ring below) measured at rest position (solid line), at -7.5 mm (dotted line) and 7 mm (dashed line)

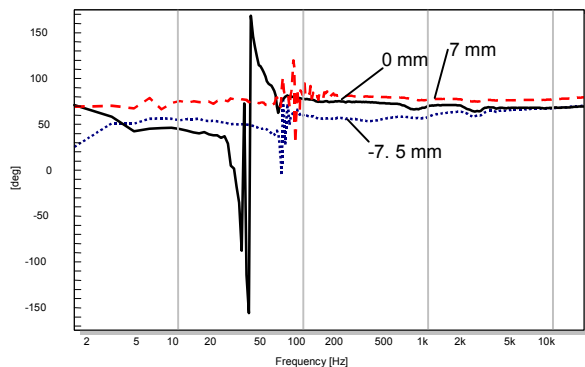


Figure 19 Phase of electrical impedance $Z_L(jw)$ of Loudspeaker 2 measured at rest position (solid line), at -7.5 mm (dotted line) and 7 mm (dashed line)

The magnitude and phase of the electrical impedance $Z_L(j\omega)$ of the second loudspeaker are shown in

Figure 18 and

Figure 19 for three coil displacements.

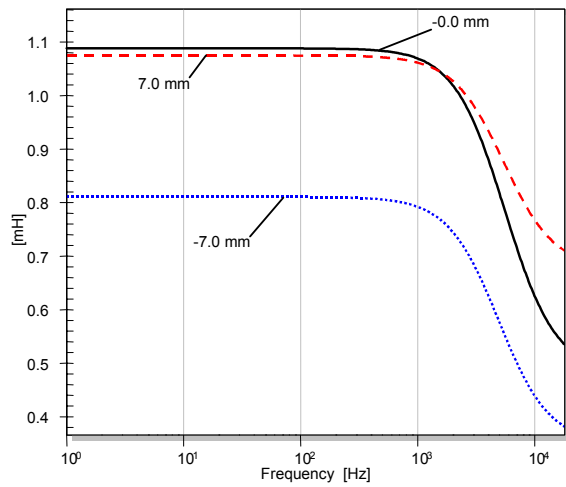


Figure 20 Effective inductance $L_{eff}(f,x)$ versus frequency f of loudspeaker 2 (ring below) plotted for the rest position (solid line) and -7 and $+7$ mm displacement (dotted and dashed line, respectively).

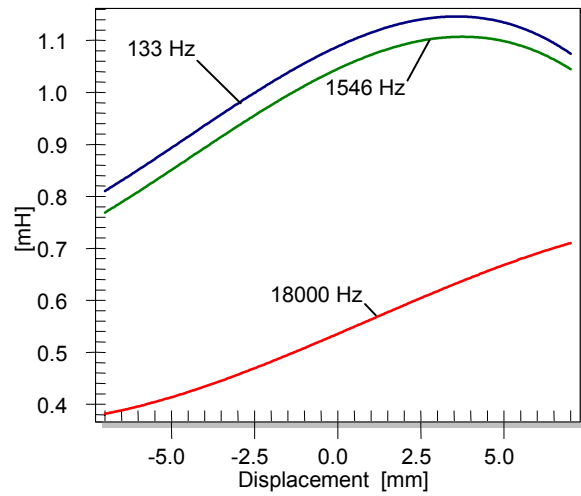


Figure 22 Effective inductance $L_{eff}(f,x)$ versus displacement x of loudspeaker 2 (ring below) plotted for frequencies 133 Hz, 1545 Hz and 18 kHz.

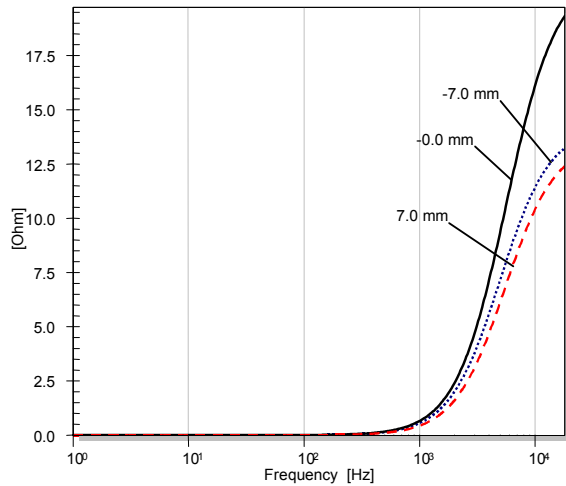


Figure 21 Effective resistance $R_{eff}(f,x)$ versus frequency f of loudspeaker 2 (ring below) plotted for the rest position (solid line) and -7 and $+7$ mm displacement (dotted and dashed line, respectively).

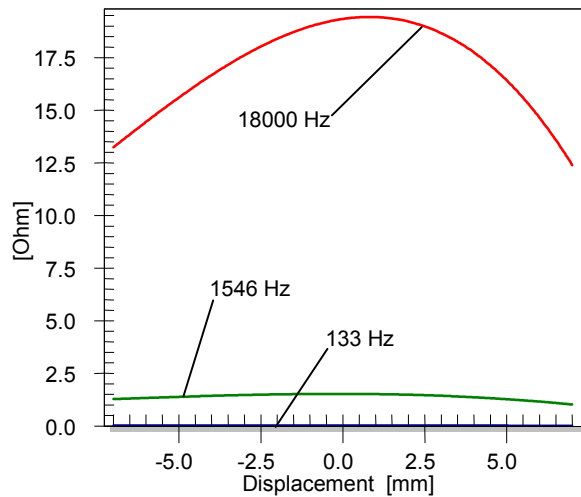


Figure 23 Effective resistance $R_{eff}(f,x)$ versus displacement x of loudspeaker 2 (ring below) plotted for frequencies 133 Hz, 1545 Hz and 18 kHz.

The effect of changing the location of the shorting ring can be seen most clearly in Figure 20 & Figure 21. Loudspeaker 1 exhibited an effective inductance which decreased as the coil moved out of the magnetic gap. This trend is close to the reverse for loudspeaker 2, the effective inductance of the coil remains almost constant as the coil moves out the gap and into free air. When the coil moves inward toward the now internally located ring, the effective inductance is seen to fall. Additionally, the phase varies significantly more with the displacement.

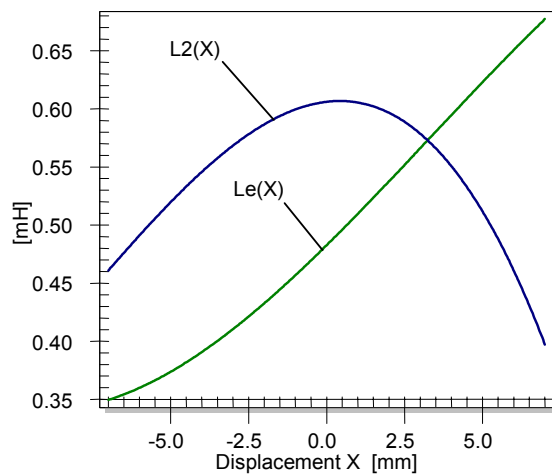


Figure 24 Inductance $L_e(x)$ and $L_2(x)$ of the loudspeaker 2 (ring below) versus displacement x .

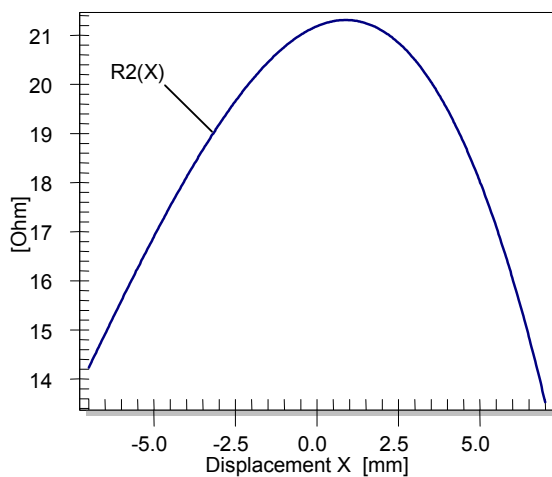


Figure 25 Inductance $R_2(x)$ of the loudspeaker 2 (ring below) versus displacement x .

Figure 24 and Figure 25 show the estimated parameters $L_e(x)$, $R_2(x)$ and $L_2(x)$ of the LR-2 model. Contrary to the parameters of loudspeaker 1 both the inductance L_2 and the shunt R_2 decay symmetrically for positive and negative displacement. The inductance $L_e(x)$ is still asymmetric but increases in an unusual way if the coil moves outwards. This is a very interesting result as it demonstrates a case where the assumption of (8) would not be valid.

4. FEM MODELING

4.1. The Use of FEM

The most obvious application of FEM is for literal modelling in which the aim is to produce a result equivalent to a measurement of some particular aspect of performance such as distortion spectra or frequency response. FEM allows the geometry and material properties to determine the behaviour by applying the appropriate physical laws. However, while this gives a wealth of information about how a loudspeaker behaves under particular circumstances it does not explain the behaviour or help to improve it.

A different approach is to represent the device with a system of analytic equations having variables representing simplified physical aspects. This parameterised approach allows the engineer to work with manageable data and to clearly identify how improvements to a design may be realised in terms of the simplified parameters. However, while this gives a clear set of specifications & targets for design or redesign it does not tell the engineer whether or how these may be achieved.

It is clearly most effective to use FEM and parameterised modelling together along with measurements to allow the reduction, as far as is possible, of the assumptions within the parameterised models through, for example, use of various FEM derived or measured transfer functions & parameters. This process essentially allows the engineer to consider a particular FEM result not alone but within the context of other physical systems & parameters and in a way to which they are accustomed. Secondly the use of the methods together allows the engineer a route from the parameters to the physical systems. Any identified parameter goals may be readily researched using the relevant FE model to investigate how or whether improvement may be achieved, and this is performed in terms of the actual physical geometry and materials of the design not comparatively arbitrary parameters.

Until FEM evolves to the extent that a model is able to fully represent all the physical systems of a loudspeaker and hardware allows physical changes to be computed in real time, linking various results & measurements using assumptions and relationships from parameter modelling is the most puissant method currently available.

4.2. Modelling Method

A discretized model of the magnet assembly was produced using the Flux2D a programme supplied by CEDRAT. The model domain was axisymmetric with second order elements. The model boundary is defined with an outer annular ‘infinite region’. In this region the elements have a modified co-ordinate system in which the outer nodes are at an infinite distance. This technique avoids the errors due to modelling only a small region of space [11][12].

Evaluating the impedance requires the current and voltage through the voice coil. This has been achieved by means of Transient Magnetic FEM in which a voltage source has been coupled to the voice coil region [11]. The result we are seeking is the current at each time step.

In the coil region of the FEM model the current is restricted to flow uniformly since the coil is a stranded conductor. In the other conductive regions the magnetic forces produced by the current are allowed to force the current flow into a skin on the surface of the conductor. The discretization is critical for this analysis and a suitable ‘skin’ of quadrilateral elements must be formed on the outer surfaces of conductive regions [11]. After sufficient time-steps for the starting transient to settle, a steady-state waveform of current versus time may be extracted from the solution files, along with the driving voltage. This analysis includes the effect of eddy currents induced in the pole and the aluminium ring; these may be seen in Figure 27 and Figure 26. The effect of the eddy currents is to produce a field opposing the voice coil flux. This has the effect of reducing the voice coil impedance.

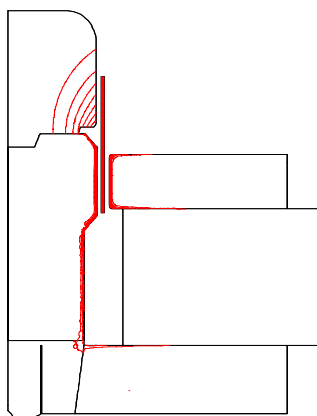


Figure 26 Loudspeaker 1. Lines of constant power density at 31.25Hz, $x=4$.

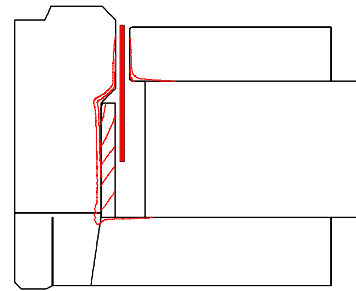


Figure 27 Loudspeaker 2. Lines of constant power density at 31.25Hz, $x=-5.75\text{mm}$

In both loudspeakers the lines of equal power density are dense in the steel pole surface and more widely spaced in the aluminium rings. This is largely due to permeability of the steel being very much higher. With increasing frequency both the extent and thickness of the skin reduce.

The current waveform flowing through the coil is extracted by evaluating the current through the coil at each timestep. A typical result is shown in Figure 28.

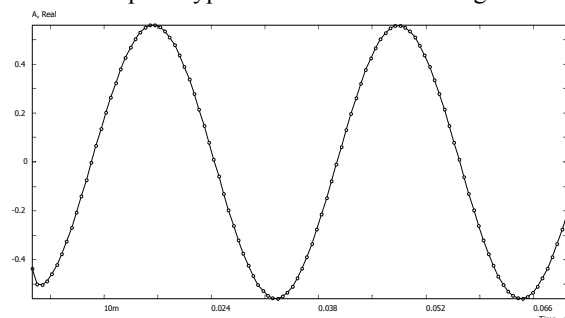


Figure 28 Current waveform for Loudspeaker 2 at 31.25Hz, $x=-5.75\text{mm}$.

Subsequently the voice coil’s ‘blocked’ electrical impedance may be calculated by applying Ohm’s law to the fundamental components of the waveforms. Each loudspeaker was solved for seven frequencies in five positions. The positions were chosen to be coincident with the measurement positions.

4.3. FEM results

Figure 29 shows the FE calculated impedance compared to the measured data for loudspeaker 1 with the coil in the rest position. At low frequencies the small errors in the modelled mechanical impedance cause some significant artefacts in the measured data. At higher frequencies the agreement is very good.

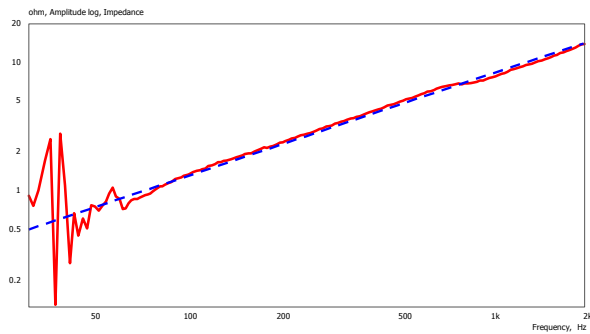


Figure 29 Example FE impedance calculation (dotted) measured data (solid). $x=0$ loudspeaker 1.

At around 1kHz the measured value is consistently below the FE value. To determine the cause of this discrepancy a conventional impedance measurement of loudspeaker 2 was made. The loudspeaker voice coil was then glued in position and a direct measurement made of the blocked impedance. The result in Figure 30 clearly shows that at 1kHz the blocked impedance is higher than the free impedance. This curious difference is thought to be an artefact resulting from the motional impedance due to non-pistonc diaphragm motion.

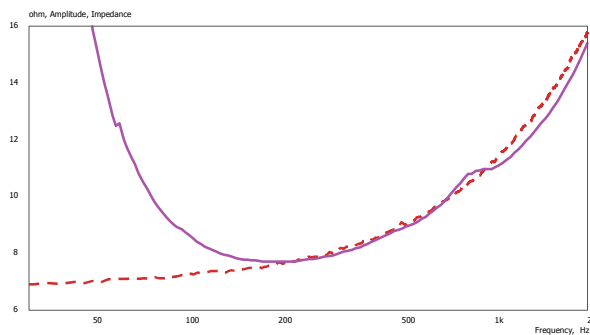


Figure 30 Conventional impedance measurement (solid) directly measured blocked impedance (dashed) loudspeaker 2.

The impedance results are illustrated opposite together with the equivalent data from the measured values using the method described in Impedance versus displacement section. To allow the large number of results to be compared contour plots have been used.

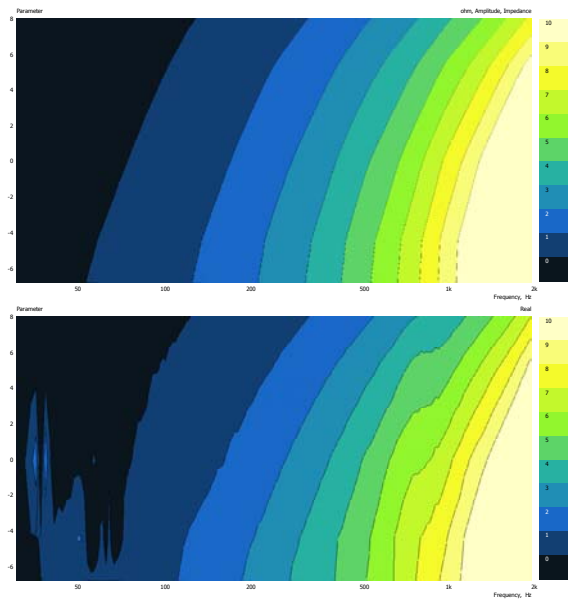


Figure 31 upper graph FEM impedance magnitude loudspeaker 1. Lower graph measured data of loudspeaker 1.

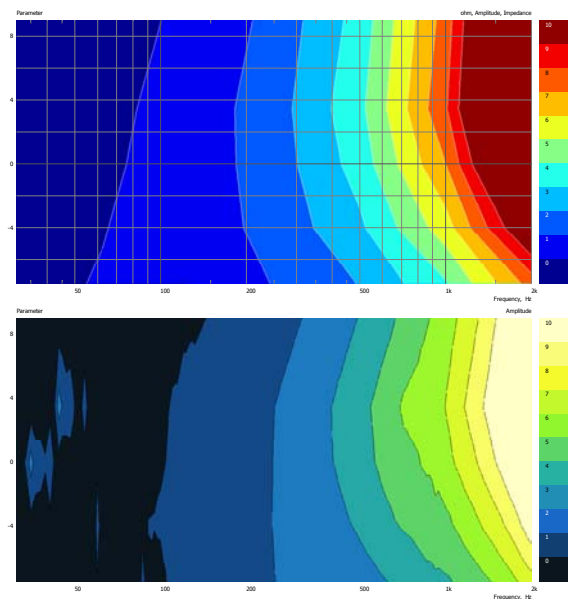


Figure 32 upper graph FEM impedance magnitude of loudspeaker 2. Lower graph measured data of loudspeaker 2.

It is evident that in both cases the FEM yields the same trend of impedance variation as the measurements. The measured data exhibits some noise around the fundamental resonance as mentioned in Excess impedance. There is also evidence of non-pistonc modal behaviour which has resulted in non-inductive impedance variations.

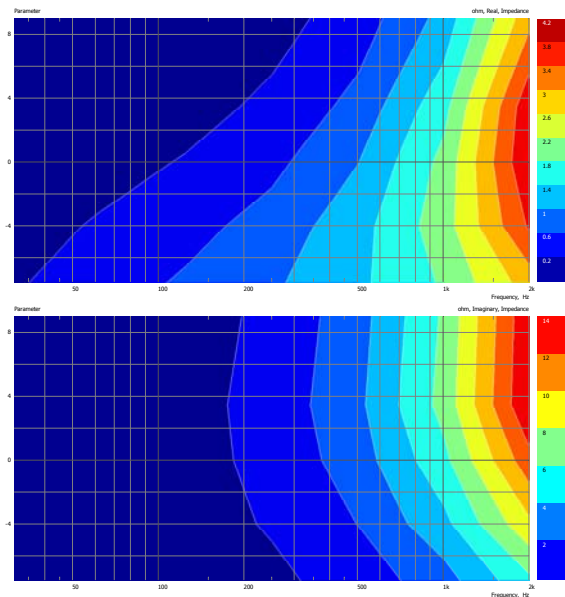


Figure 33 Loudspeaker 2 upper graph real part of FEM impedance. lower graph imaginary part of FEM impedance.

Figure 33 shows the real and imaginary parts of the FEM derived impedance for loudspeaker 2. The difference in symmetry of the impedance mentioned in Non-linear Parameters can be clearly seen.

5. PREDICTION OF DISTORTION

5.1. Analytic prediction

If non-linear parameters of the equivalent circuit in Figure 1 are measured then the state signal (current, displacement) and the sound pressure output can be predicted for any excitation signal. This technique is useful for several applications: diagnostic testing of a loudspeaker; assessment or improvement of a new design; auralization of large signal performance with music or other test signals [1]. The Simulation module (SIM) [13] has been used to predict the distortion based upon the measured non-linear parameters $L_c(x)$, $R_2(x)$ and $L_2(x)$ above.

The results of these simulations may be directly compared with the results of the 3D Distortion measurement module (DIS) [14] which provide a direct measure of the actual distortion of the loudspeaker. In this way we are able to validate the measured non-linear parameters of the LR-2 model by comparing predicted and measured distortion generated in the input current.

Measurement of distortion in the electrical input current reveals the distortion generated by the varying input impedance almost directly (provided the loudspeaker is connected to an amplifier with a suitably low output impedance). The distortion generated in the current will also appear in the displacement, velocity and sound pressure output. However, the distortion generated by displacement varying force factor $Bl(x)$ and compliance $C_{MS}(x)$ appear in the current only close to the resonance where the velocity and back EMF are high. Doppler distortion and any other radiation distortion will not be detected in the input current.

A very important aspect is the selection of the test stimulus. A single tone reveals only harmonic distortion which is, for displacement varying input impedance $Z_L(j\omega, x)$, relatively low. This is because at low frequencies the variation of $Z_L(j\omega, x)$ with displacement x is relatively small, seen in Figure 10 and

Figure 18 for both loudspeakers. In addition at high frequencies the voice coil displacement becomes very small and the variation of $Z_L(j\omega, x)$ with displacement is minimal.

However, a two-tone signal comprising a bass tone at frequency f_2 and a probe tone at higher frequency f_1 is a much more revealing signal [15]. The bass tone is set to a fixed frequency below resonance to produce a large displacement of ~ 5 mm peak. The second 'probe' tone is varied from 200Hz to 18 kHz to represent any audio signal in the pass-band of the loudspeaker. The varying impedance Z_L generates not only harmonics of both tones but additionally difference and summed-tone intermodulation components, which may exceed the harmonics significantly.

There is a simple relationship between shape of a non-linear parameter and the order of the resulting distortion component. A distinct asymmetry of the parameter, such as in Figure 16 and Figure 17, will generate dominant 2nd order distortion, which will outweigh 3rd order and higher distortion. Conversely a symmetrical curve, such as in $L_2(x)$ and $R_2(x)$ in Figure 24 and Figure 25, will generate strong 3rd-order and other odd-order distortion components.

5.2. FEM prediction

The FE provides an alternative means of predicting the distortion. Using the FEM software a full kinematic solution for an arbitrary input signal may be computed. This solution can again be used to predict the distortion, this time from FE models adapted from those developed

in order to model the voice coil impedance. For the purpose of this paper, this type of FEM solution appears for only one frequency; the solution time is very long and use of this type of modelling is thus restrictive. The two-tone intermodulation stimulus must be solved with a small time step defined by the higher frequency over two periods of the lower frequency, provided that the frequencies are integral multiples. It is estimated that solving with a two-tone intermodulation stimulus for the seven octave spaced frequencies up to 2kHz would take 180 hours of processor time on a 2GHz PC.

As we have seen, the results of the FE correlate well with measured $Z_L(j\omega, x)$. The use of the measured non-linear parameters to calculate the distortion is dependent upon the LR-2 fitting and the assumption that the model is adequate to describe the behaviour of the system. Additionally, as previously discussed, the measurement method (quasi-static) may have a bearing upon the deduction of the LR-2 parameters and indeed the measured $Z_L(j\omega, x)$. The full kinematic analysis does not have these limitations as it returns directly to the fundamental physical relationships in order to calculate the system output. It is also able to account for more complex phenomena such as the effect of current magnitude on the impedance response. The FE allows application of specific laws of physics to model the behaviour whereas the parameterised model matches specific effects in such a way that the resulting non-linear system of equations behaves in a closely similar way to the loudspeakers measured behaviour. The FE method used here is also able to represent other non-linear relationships using user prescribed power series. This facility could be used to model the $C_{ms}(x)$ non-linearity for example.

It would be possible to use the $Z_L(j\omega, x)$ results from FEM to determine the LR2 parameters and predict the distortion with the SIM module. This has not been done here since the results would be derived from almost identical data. In practice the time saving of this method is substantial and it is anticipated that further work will be done using this method. Where further understanding of the physics is an aim the detailed results of a direct FEM approach are likely to outweigh the time cost.

5.3. Results

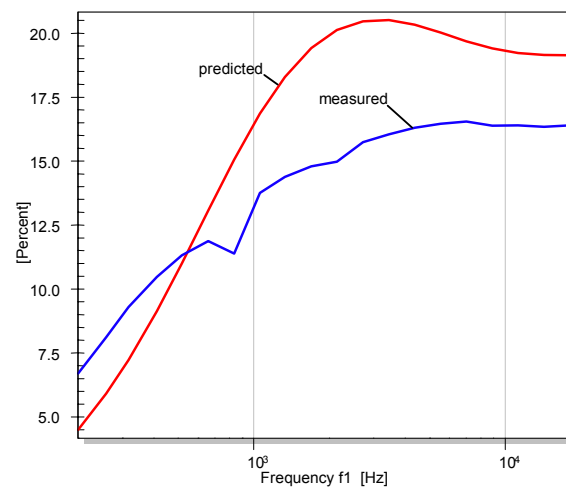


Figure 34 Second –order intermodulation distortion in the input current measured and predicted by using the parameterized method (SIM) for loudspeaker 1

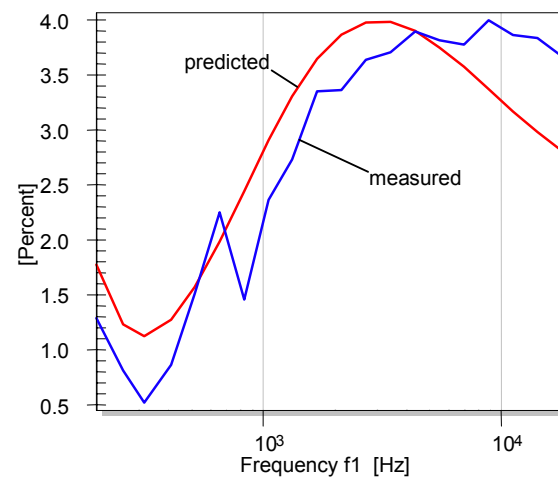


Figure 35 Third –order intermodulation distortion in the input current measured and predicted by using the parameterized method (SIM) for loudspeaker 1

Figure 34 and Figure 35 show the measured and predicted 2nd-order and 3rd-order distortion for loudspeaker 1. The 2nd-order distortion is dominant and is caused by asymmetry of the parameters $L_e(x)$, $L_2(x)$ and $R_2(x)$.

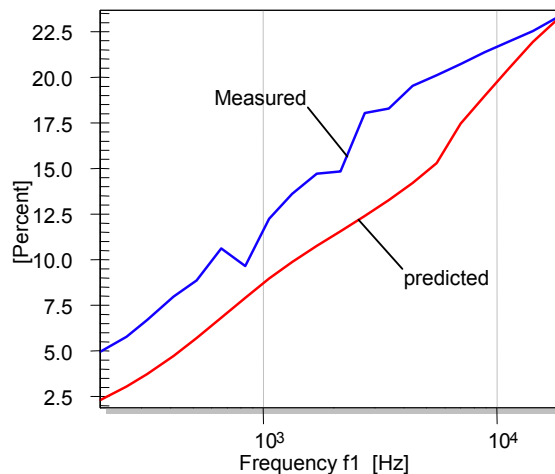


Figure 36 Second-order intermodulation distortion in the input current and predicted by using the parameterized method (SIM) for loudspeaker 2 (ring below)

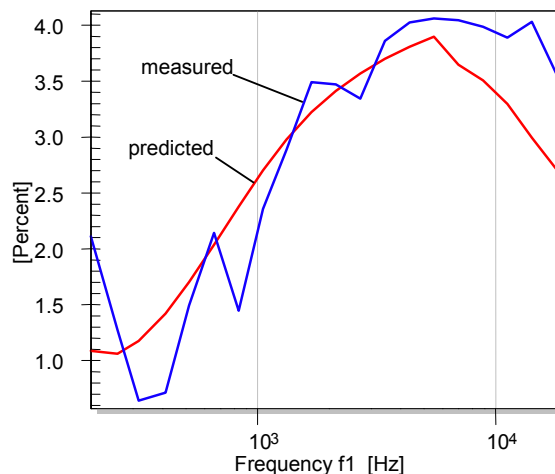


Figure 37 Third-order intermodulation distortion in the input current measured and predicted by using the parameterized method (SIM) for loudspeaker 2 (ring below)

Loudspeaker 2, with shorting ring below the gap, gives a slightly better performance than loudspeaker 1 for frequencies below 1 kHz. Here the 2nd-order distortion components are smaller but still dominant as the asymmetry remains in the non-linear parameters. At high frequencies the loudspeaker 2 generates similar distortion levels to loudspeaker 1 which corresponds with the increasing asymmetry of the effective inductance $L_{\text{eff}}(x, j\omega)$ in Figure 22.

Note that the distortion increases with frequency similarly to the increase in the variation of the impedance Z_L with x shown in Figure 10.

#FE DISTORTION RESULTS#

6. CONCLUSION

Detailed knowledge of the inductive behaviour is essential for the design of loudspeakers with minimal distortion.

Modern (full kinematic) FE methods are able to show the relationship between geometry, material properties on one side and the final behaviour (linear and nonlinear distortion) on the other side on principle. FE can also be applied to conceptual loudspeakers.

However, describing the loudspeaker output by one FE model considering all electrical, mechanical and acoustical mechanisms has some practical disadvantages. Solving such a complex FE model is still time consuming and depends on many (unknown) parameters. A lumped parameter model may be a link between geometry and performance. As shown for the voice coil impedance the most important information can be compressed in a few number of meaningful parameters depending on the model (LR2, Leach, Wright). The LR2 or an extended model with more RL cascades (LR3) is the best candidate to consider the variation versus displacement. Loudspeaker 2 impedance results show that all LR2 parameters must vary independently with x to satisfactorily describe the nonlinear behaviour of some loudspeakers over the full frequency range .

In the paper the parameters describing the voice coil impedance have been measured by using a new quasi static technique and modelled by using FE, with exceptional agreement. It is possible to investigate the effect of the shorting rings and to derive other indications for improvements.

After verifying the lumped electrical parameters calculated by a first FE a more complex FE considering other mechanical or acoustical parts may be used to predict the loudspeaker output. However, an interesting alternative is to use here a numerical integration (SIM module) of the nonlinear differential equation based on the identified lumped parameter model.

The close connection between measurement and simulations based on both parameterized methods, FE BEM and other discrete techniques are invaluable. . This gives the engineer a full picture not only of the complicated voice coil impedance but also on other mechanical and acoustical mechanics in loudspeakers.

7. REFERENCES

- [1] W. Klippel, "Prediction of Speaker Performance at High Amplitudes", Presented at the 111th Convention of the Audio Engineering Society, preprint 5418, November 2001. J. Audio Eng. Soc., Vol. 49, No. 12, p. 1216, December 2001.
- [2] #####
- [3] J.Vanderkooy, "A Model of Loudspeaker Driver Impedance Incorporating Eddy Currents in the Pole Structure" J. Audio Eng. Soc., Vol. 37 No 3 pp. 119-128; March 1989.
- [4] M. Dodd, "The Development of a Forward Radiating Compression Driver by the Application of Acoustic, Magnetic and Thermal Finite Element Methods," Presented at the 115th Convention of the Audio Engineering Society, preprint 5886, September 2003.
- [5] "Manual of the KLIPPEL Analyzer System", Klippel GmbH, www.klippel.de, 2004.
- [6] W.M. Leach, "Loudspeaker voice-coil inductance losses: circuit models, parameter estimation, and effect on frequency response", J. Audio Eng. Soc., Vol. 50, No. 6, 2002.
- [7] J.R. Wright, "An empirical model for loudspeaker motor impedance", J. Audio Eng. Soc., Vol. 38, No. 10, 1990.
- [8] "Large Signal Identification (LSI)", Specification of the KLIPPEL Analyzer module, Klippel GmbH, www.klippel.de, 2003.
- [9] "Maximizing LPM Accuracy", Application note AN 25 of the KLIPPEL Analyzer System, Klippel GmbH, www.klippel.de, 2004.
- [10] "Processing Software (MAT)", Specification of the KLIPPEL Analyzer module, Klippel GmbH, www.klippel.de, 2003.
- [11] M.A. Dodd, "The Transient Magnetic Behaviour of Loudspeaker Motors" Presented at the 111th Convention of the Audio Engineering Society, preprint 5410, November 2001.
- [12] FLUX2D 7.60 User Manual, CEDRAT, Meylan France, 2002.
- [13] "Simulation (SIM)", Specification of the KLIPPEL Analyzer module, Klippel GmbH, www.klippel.de, 2003.
- [14] "3D Distortion Measurement (DIS)", Specification of the KLIPPEL Analyzer module, Klippel GmbH, www.klippel.de, 2003.
- [15] W. Klippel, "Assessment of voice-coil peak displacement X_{max} ", J. Audio Eng. Soc., Vol. 51, No. 5, pp. 307-324, 2003.